Low-cost generation of RF test stimuli from baseband digital signals

Kamilia Tahraoui, Thibault Vayssade, François Lefèvre, Laurent Latorre, Florence Azaïs

Version submitted by the authors

Low-cost generation of RF test stimuli from baseband digital signals

K. Tahraoui
LIRMM, Univ. Montpellier, CNRS
Montpellier, France
kamilia.tahraoui@lirmm.fr

T. Vayssade
LIRMM, Univ. Montpellier, CNRS
Montpellier, France
thibault.vayssade@lirmm.fr

F. Lefevre
NXP Semiconductors
Caen, France
francois.lefevre@nxp.com

L. Latorre
LIRMM, Univ. Montpellier, CNRS
Montpellier, France
laurent.latorre@lirmm.fr

F. Azaïs
LIRMM, Univ. Montpellier, CNRS
Montpellier, France
florence.azais@lirmm.fr

***Abstract*— This paper targets reduction of RF testing costs, focusing in particular on the generation of modulated stimuli for testing the reception chain of RF communication devices. It proposes an innovative low-cost solution that can be implemented on a standard digital Automated Test Equipment (ATE). The approach relies on the generation of a baseband digital signal with specific encoding, and the exploitation of one of its harmonic replicas as RF test stimulus. Spectral integrity of the signal around the targeted harmonic replica is ensured through a careful selection of the ATE sampling frequency. A generic methodology for practical implementation is presented and illustrated in this paper considering two popular digital modulation formats, namely Binary Phase-Shift Keying (BPSK) and Minimum-Shift Keying (MSK). Experimental validation is performed using a microcontroller unit (MCU) capable of operating at a sampling rate up to 500Mbps. Results show that despite the limited sampling capability of the equipment, test stimuli with the desired spectral characteristics in the 433MHz and 868MHz ISM bands can be generated, validating the proposed solution.**

Keywords*— Analog/RF test; test stimulus generation; digital ATE; sampling theory; BPSK modulation

I. INTRODUCTION

With the popularization of wireless applications, there is a pressing need to develop new solutions for testing communication devices with low-cost instrumentation. Indeed, the conventional approach to test RF front-end modules relies on the use of an ATE equipped with specific instruments that can generate or analyze RF modulated signals. This complex instrumentation is extremely expensive and constitutes a major contributor to RF testing costs.

One approach to reduce test costs is to develop solutions that relax constraints on the required instrumentation so that a low-cost tester can be used, preferably a digital tester, as this will enable the digital part of a System-on-Chip (SoC) to be tested using the same test infrastructure as the RF part. A number of works targeting the development of digital solutions can be found in the literature, some focusing on complete transceivers [1-3] while others concentrate on the transmit chain [4,5] or the receive chain [6-11]. Among works that concentrate on the receive chain, some are more specifically oriented towards solutions that use a binary signal as test stimulus to enable compatibility with standard digital ATE. Two approaches can be distinguished, i.e. the generation of binary signals optimized to determine RF performance parameters based on a model of the Device Under Test (DUT) [6,7], or the generation of binary signals representative of RF test stimuli used in conventional testing [9,10]. In this work, we focus on the generation of baseband binary signals representative of RF test stimuli used for receiver sensitivity testing, enabling implementation on a standard digital ATE.

This paper is organized as follows. The characteristics of the targeted RF test stimuli are introduced in Section II. The principle and the fundamental concepts of the proposed strategy are presented in Section III. Practical implementation is discussed in section IV and demonstrated through hardware measurements in Section V. Finally, Section VI concludes the paper and presents directions for future work.

II. TARGETED TEST STIMULUS CHARACTERISTICS

To illustrate the applicability of the proposed solution, we consider two popular digital modulation schemes belonging to the categories of Phase-Shift Keying (PSK) and Frequency-Shift Keying (FSK), namely Binary Phase-Shift Keying (BPSK) and Minimum-Shift Keying (MSK). The main features of these modulation schemes are summarized in this section.

In its general form, an angle-modulated signal can be written as:

$$x(t) = A\cos\big(\Omega(t)\big) = A\cos(\omega_c t + \phi(t)) \quad (1)$$

where $\Omega(t)$ is the instantaneous phase of the modulated signal, A is the amplitude of the carrier signal, ω_c is the angular frequency of the carrier signal, and $\phi(t)$ is the instantaneous phase deviation. The modulation scheme determines how the instantaneous phase deviation $\phi(t)$varies.

In case of PSK, the instantaneous phase deviation can take only discrete values ϕ_n separated by $\Delta\phi = 2\pi/M$ depending on the binary data to be transmitted, where M is the number of discrete phases. The time-domain expression of the instantaneous phase deviation is therefore simply given by:

$$\phi_{PSK}(t) = \phi_n = (n-1)\Delta\phi \quad for \;\; kT_b \le t \le (k+1)T_b \;\; n = 1,2,\dots M \quad (2)$$

where T_b is the bit duration.

BPSK is a special case of PSK where $M = 2$, i.e. only two discrete phase values separated by $\Delta\phi = \pi$ are used, with classically $\phi_0 = 0$ and $\phi_1 = \pi$. In this case, the instantaneous phase deviation can be expressed with:

$$\phi_{BPSK}(t) = \Delta\phi \cdot b_k \quad for\; kT_b \le t \le (k+1)T_b \quad (3)$$

where $b_k \in \{0,1\}$ is the binary value of the kth data bit.

The frequency domain expression of a BPSK signal is given by [11]:

$$S_{BPSK}(f) = \frac{A}{2}\frac{sin[\pi(f-f_c)T_b]}{\pi(f-f_c)\sqrt{T_b}} = \frac{A\sqrt{T_b}}{2}\, sin_c[(f-f_c)T_b] \quad (4)$$

In case of FSK, it is the instantaneous frequency of the carrier signal that is shifted between discrete frequencies depending on the binary data to be transmitted. In general, only two discreate frequencies $f_0 = f_c - \Delta f$ and $f_1 = f_c + \Delta f$ are used, and phase continuity is ensured to avoid wideband frequency components. The time-domain expression of the instantaneous phase deviation for a continuous-phase FSK signal is given by:

$$\phi_{FSK}(t) = \pi h \frac{a_k(t - kT_b)}{T_b} + \pi h \sum_{n=0}^{k-1} a_n \quad for \quad kT_b \le t \le (k+1)T_b \tag{4}$$

where h is the modulation index and $a_k = \pm 1$ corresponds to the NRZ version of the k[th] data bit b_k. The first term corresponds to the constant frequency deviation Δf of the continuous-phase FSK signal while the second term represents the accumulated phase. The frequency deviation is related to the modulation index with $\Delta f = h/2T_b$.

The frequency domain expression of a continuous-phase FSK signal is given by [11]:

$$S_{FSK}(f) = \frac{A\sqrt{T_b}}{2\pi} \frac{h}{(2F)^2 - h^2} \cdot \frac{\cos(\pi h) - \cos(2\pi F)}{[(\cos(\pi h) - \cos(2\pi F))^2 + \sin^2(2\pi F)]^{1/2}} \tag{5}$$

where $F = (f - f_c)T_b$ is the normalized frequency.

MSK is a special case of continuous-phase FSK where the modulation index is chosen as $h = 0.5$. It corresponds to a spectrally efficient form of FSK, where the difference between the higher and the lower frequencies is equal to half the bit rate. In this case, the expression in the frequency domain simplifies to:

$$S_{MSK}(f) = \frac{2A\sqrt{T_b}}{\pi} \frac{cos[2\pi(f - f_c)T_b]}{1 - [4(f - f_c)T_b]^2} \tag{6}$$

Figure 1 gives the spectrum of BPSK and MSK signals as a function of the normalized frequency. It can be observed that the MSK spectrum exhibits a main lobe narrower than the BPSK spectrum and a higher fall off rate. In particular, the null-to-null bandwidth (i.e. the width of the main lobe) is $1.5/T_b$ for MSK and $2.0/T_b$ for BPSK, and the fall-off rate is proportional to the normalized frequency at the power of 4 for MSK and at the power of 2 for BPSK. As a result, the BPSK spectrum has a much larger bandwidth than that of the MSK spectrum. The bandwidth containing 99% of the power can be obtained by numerical calculations; for these two modulation schemes, the result is as follows [12]:

$$BW_{99\%-BPSK} = 20.56\, R_b\,, \quad BW_{99\%-MSK} = 1.18\, R_b \tag{7}$$

where $R_b = 1/T_b$ is the data rate.

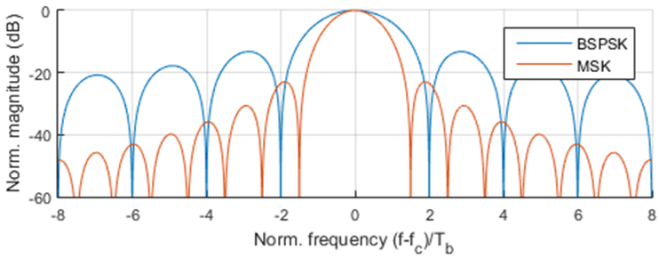

Fig. 1. Theoretical spectrum of BPSK and MSK signals

These two specific cases of PSK and FSK were selected in this paper to illustrate the ability of the proposed technique to handle various modulation formats with different characteristics in terms of bandwidth and spectral content.

III. Digital Test Stimulus Generation

A. Principle

Our proposal to reduce the testing costs of receivers is to use a 1-bit signal generated by a standard digital tester channel as test stimulus. This signal should be defined such that its spectral characteristics are similar to the spectral characteristics of the conventional stimulus generated by an RF tester channel over a given frequency band, i.e. the frequency band of interest for the DUT. In this approach, it is assumed that DUT has a narrow band, which is the case of receivers, and therefore out-of-band components are acceptable since they will be filtered by the DUT itself. Alternatively, a filter centered on the DUT frequency band may be placed on the load board that provides the interface between the ATE and the DUT, if required.

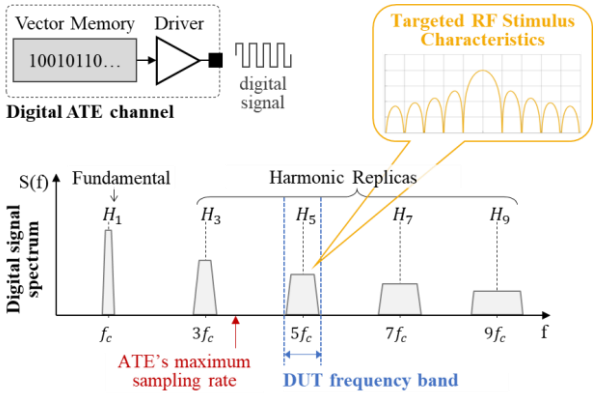

Fig. 2. Strategy for RF test stimulus generation from baseband digital signal

One of the major limitations imposed by the test equipment is that the range of frequencies that can be reached for the digital signal is limited to half the ATE's maximum sampling rate (Nyquist), which might not be sufficient to address the DUT frequency band. To cope with this issue, the idea is to exploit high frequency components of the digital signal, following the same approach than in [6] where a pulse sequence optimized by a genetic algorithm is used as test stimulus. In our case, the 1-bit signal will be defined as a digital carrier modulated with a specific encoding, the frequency of the digital carrier being compatible with the sampling capabilities of the ATE. As illustrated in Figure 2, such a digital signal exhibits harmonic replicas located around multiples of the fundamental frequency (odd multiples only if the digital carrier has a 50% duty cycle); it is therefore possible to reach frequencies beyond the ATE's maximum sampling rate. The idea is then to exploit one of these harmonic replicas as test stimulus. To this end, the frequency of the digital signal should be set such that the selected harmonic replica is centered on the DUT frequency band of interest, i.e. $f_c = f_{c_{target}}/i$, where f_c is the carrier frequency of the digital signal, $f_{c_{target}}$ is the carrier frequency of the targeted RF stimulus and i is the order of the selected harmonic replica.

The first challenge to be solved for the practical implementation of this strategy is to encode the digital signal such that its spectral characteristics are representative of the targeted RF test stimulus, over the frequency band of interest. In order to understand how the harmonic replicas are related to the digital signal spectrum around the fundamental frequency (hereafter referred to as the baseband spectrum), a preliminary study has been conducted in [10] considering a

simple analog modulation scheme, i.e. single-tone Frequency or Phase Modulation (FM/PM). This analysis is extended in this paper to the case of digital modulation formats.

The second challenge is related to the hardware architecture of a digital tester, which is a sampled-time system. The sampled-time generation process introduces a periodization of the spectrum, with the creation of copies of the original spectrum (called images) shifted by multiples of the sampling frequency. In our specific context, the original spectrum is a complex one composed not only of a baseband spectrum but also of harmonic replicas. Depending on the chosen sampling frequency, some images of the baseband spectrum and/or harmonic replicas are susceptible to interact with the selected harmonic replica, altering its spectral content. The second challenge is therefore to identify appropriate sampling conditions to ensure the preservation of the spectral characteristics around the selected harmonic replica. This aspect is addressed through the computation of a corruption estimator described in Section C.

In summary, the main features of the proposed strategy for low-cost generation of RF test stimuli are:

- exploitation of a harmonic replica of a low-frequency binary signal generated with a standard digital tester channel in order to obtain a signal at higher frequency,
- specific encoding of the baseband digital signal such that the spectral characteristics around the selected harmonic replica are representative of the targeted RF test stimulus,
- appropriate choice of the sampling frequency such that the spectral characteristics around the selected harmonic replica are not altered by images of the original spectrum.

It is worth pointing out that this strategy differs from the approach adopted in [8], where an image of a sampled analog signal is exploited to obtain a higher-frequency signal. In our case, the signal generated is purely digital, thus avoiding the use of a digital-to-analog converter (DAC). Furthermore, it is a harmonic replica of the digital signal that is exploited to obtain a signal at higher frequency, and interaction between images of the sampled binary signal and the selected harmonic replica is avoided by means of an appropriate choice of sampling frequency.

B. Encoding of the baseband digital signal

The starting point of the definition of the digital signal is to consider a modulated analog signal x(t) as defined by Eq.1, submitted to a zero-crossing operation. The resulting signal $y(t)$ is a binary signal that can be expressed as an infinite sum of modulated analog signals:

$$y(t) = sgn[x(t)] = \frac{4}{\pi}\left(A\cos(\Omega(t)) + \frac{A}{3}\cos(3\Omega(t)) + \frac{A}{5}\cos(5\Omega(t)) + \cdots\right) \quad (8)$$

where $\Omega(t)$ is the instantaneous phase of the original modulated analog signal and A is the amplitude of the digital signal. The first term corresponds to the baseband component of the digital signal while the following terms corresponds to the harmonic replicas located at odd multiples of the baseband frequency.

Introducing $\Omega(t) = \omega_c t + \phi(t)$ in Eq.8, it comes:

$$y(t) = \frac{4}{\pi}\sum_i \frac{A}{i}\cos(i\omega_c t + i\phi(t)) \quad for\ i = 1,3,5,\ldots \quad (9)$$

This expression indicates that the digital signal resulting from a zero-crossing operation can be considered as an infinite sum of modulated analog signals with a modification of both the amplitude and the instantaneous phase deviation for each individual modulated analog signal. In terms of spectral content, the baseband spectrum has the same characteristics than the original analog signal; however, each harmonic replica has different characteristics, the instantaneous phase deviation being multiplied by the harmonic replica order. In order to achieve the desired spectral characteristics around a given harmonic replica, the digital signal should therefore be encoded such that $\phi(t) = \phi_{target}(t)/i$, where $\phi_{target}(t)$ is the instantaneous phase deviation corresponding to the targeted modulation scheme and i is the order of the selected harmonic replica.

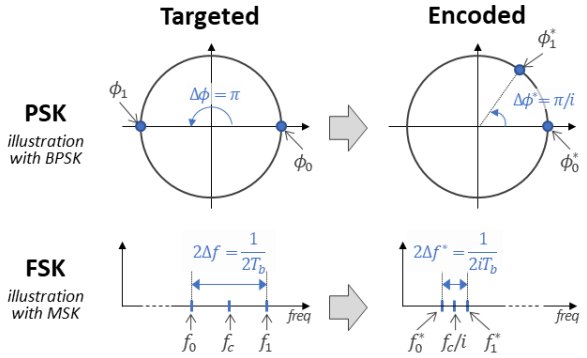

Fig. 3. Encoding of the baseband digital signal

Concretely, the analog signal that serves for the computation of the digital signal should be defined as follows:

- In case of PSK, the instantaneous phase deviation depends on the separation $\Delta\phi$ between the discrete phase values as indicated by Eq.2; the analog signal should therefore be defined with:

$$\Delta\phi^* = \frac{\Delta\phi_{target}}{i} = \frac{2\pi}{iM} \quad (10)$$

  where $\Delta\phi_{target}$ is the phase separation corresponding to the targeted PSK scheme. This equation is valid for any PSK scheme, including BPSK with $M = 2$ and $\Delta\phi_{BPSK} = \pi$, and QPSK with $M = 4$ and $\Delta\phi_{QPSK} = \pi/2$. However, the modification of $\Delta\phi$ might be omitted in case of BPSK with $\phi_0 = 0$ and $\phi_1 = \pi$. This is a particular case where the multiplication of the original phase separation $\Delta\phi_{BPSK}$ by an odd multiple leads to the same ϕ_0 and ϕ_1 values, taking into account 2π modulus; in all other cases, the modification of $\Delta\phi$ is mandatory. Note that the signal defined with $\Delta\phi^*$ does not correspond to a conventional analog modulated signal since the discrete phases are no longer distributed over the entire trigonometric circle, but occupy only a limited portion, as illustrated in Figure 3.
- In case of FSK, the instantaneous phase deviation is a function of the modulation index h as indicated by Eq.4, which is directly related to the frequency deviation Δf; the analog signal should therefore be defined with:

$$\Delta f^* = \frac{\Delta f_{target}}{i} = \frac{h_{target}}{2iT_b} \quad (11)$$

  where h_{target} is the modulation index of targeted modulation scheme.

As an illustration of this encoding process, let us consider the case where the 3rd-order harmonic replica is used to generate a BPSK and MSK test stimulus. The analog signal that serves for the generation of the digital signal is defined with $\Delta\phi^* = \pi/3$ for BPSK and $\Delta f^* = 1/12T_b$ for MSK.

The spectrum of the digital signal resulting from the zero-crossing of the analog signal is shown in Figure 4.a and 4.b, respectively for BPSK and MSK (close-up view around the baseband spectrum and the first two odd harmonic replicas). In both cases, the spectral content of the 3rd-order harmonic replica matches with the targeted one, while the baseband spectrum and the 5th-order harmonic replica exhibit very different characteristics.

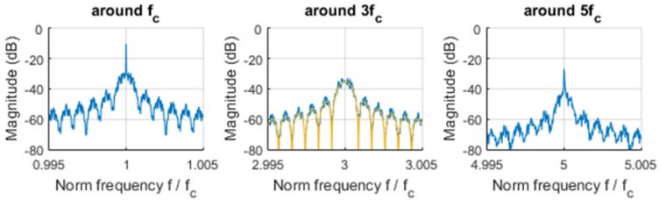

(b) BPSK test stimulus

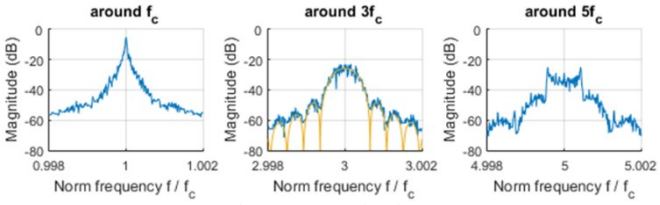

(b) MSK test stimulus

Fig. 4. Zoom around the baseband sprectrum and first two odd replicas of the digital signal for test stimulus generation using 3rd-order harmonic replica

C. Choice of the sampling frequency

In our specific context, the digital signal will be generated by digital tester channel and will not directly correspond to the digital signal obtained from a zero-crossing operation on an analog signal. Indeed, the generation of a signal with an ATE digital channel involves the sequential reading of logic values stored in the vector memory and the formatting of these data into an electrical signal, where a level V_{iL} is associated to a logic 0 and a level V_{iH} to a logic 1, each level being maintained until the next data for a duration set by the tester period $T_{cycle} = 1/f_s$. The actual digital signal delivered by a digital tester channel therefore corresponds to a sampled-and held version of the digital signal defined in the previous subsection, with transitions that occur on a discrete-time grid determined by the ATE sampling frequency f_s.

The spectral characteristics of the actual digital signal differ from the theoretical one in two aspects: (i) the spectrum comprises not only the baseband spectrum and harmonic replicas but also images of these components due to the sampling process, and (ii) the amplitude of frequency components is shaped by the sin_c function due to the hold process.

As an illustration, Figure 5 shows the spectrum of a pure square-wave signal obtained from zero-crossing operation applied on a sine-wave signal and the spectrum of the sampled-and-held version with $f_s = 4.3f_c$. The global shaping introduced by the sin_c function is clearly visible, with a cancellation of all components close to the local zeros present at every multiple of the sampling frequency. The expected harmonic tones located at odd multiples of the signal frequency are present but they are mixed with other components of similar or even higher amplitude. The components of high amplitude actually correspond to high-frequency images of the fundamental and harmonic tones located below the Nyquist frequency, while the other additional components correspond to low-frequency images of the harmonic tones located above the Nyquist frequency.

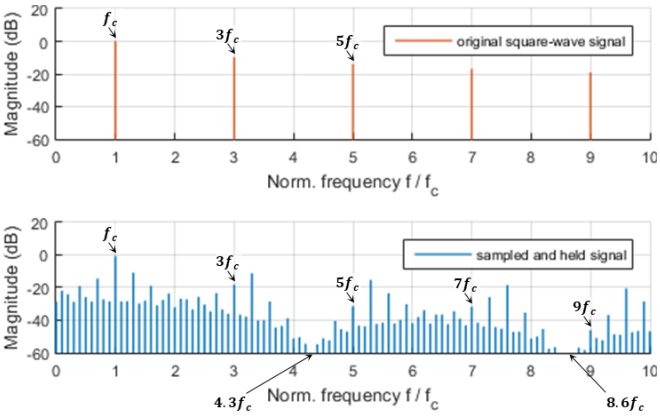

Fig. 5. Spectrum comparison between pure square-wave signal and sampled-and-held signal with $f_s = 4.3f_c$

In the context of the proposed strategy, the presence of these additional components is not a problem as long as they do not fall in the DUT frequency band. The location and the amplitude of these additional components directly depends on the chosen value of the sampling frequency f_s. A major challenge is therefore to identify favorable sampling conditions, i.e. values of f_s that ensures that no image of significant magnitude fall within the frequency band of interest. To this end, a corruption estimator was defined in [10], which permits to evaluate how much the power contained in a given frequency band around the selected harmonic deviates from the power of an ideal square-wave:

$$Corr\ Est_i = \frac{\left|EBP_i - HCP_i^{expected}\right|}{HCP_i^{expected}} \quad (12)$$

where HCP stands for Harmonic Carrier Power and EBP for Enlarged Bandwidth Power. The computation of this estimator is based on an analytical expression of a sampled-and-held digital carrier; refer to [10] for more details.

In this work, we will use the corruption estimator to identify the most favorable sampling condition. Practically, the corruption score will be computed for all sampling frequencies compatible with the equipment's capabilities; the chosen sampling frequency will be the one that leads to the minimum score.

IV. Implementation

A. Methodology

Based on the fundamental concepts defined in the previous section, we describe in this section the methodology for practical implementation of the proposed solution. For a given application, the input parameters are on the one hand the characteristics of the targeted RF test stimulus in terms of frequency ($f_{c_{target}}$), data rate (R_b) and modulation format ($\Delta\phi_{target}$ for PSK and Δf_{target} for FSK), and on the other hand the characteristics of the test equipment in terms of maximum sampling rate ($f_{s_{max}}$) and frequency resolution (Δf_s). The methodology involves three main steps, as detailed hereafter.

The first step is to select the order of the harmonic replica exploited as RF test stimulus. The main requirement is that the baseband frequency of the digital signal $f_c = f_{c_{target}}/i$ should comply with the Nyquist criterion, taking into account the maximum sampling capability of the test equipment, which can be expressed by:

$$i \geq 2f_{c_{target}}/f_{s_{max}} \quad (13)$$

The selected harmonic replica H_i corresponds to the smallest odd value of i that satisfies this equation.

The second step is to choose a sampling frequency that avoid the presence of images with significant magnitude in the DUT frequency band. For this, the corruption estimator is computed for all possible f_s values between the Nyquist frequency $f_{s_{min}} = f_{c_{target}}/2i$ and the maximum sampling frequency $f_{s_{max}}$, taking into account the frequency resolution Δf_s of the equipment. The sampling frequency with the lowest corruption score is selected.

The final step is to determine the content of the binary sequence that will be stored in the ATE vector memory. As illustrated in Figure 6, the sequence is derived from a modulated analog signal submitted to zero-crossing and sampling operations. More precisely for a given input message, the modulated analog signal is computed as $x(t) = cos(2\pi f_c t + \phi^*(t))$, where the instantaneous phase deviation $\phi^*(t)$ is defined by Eq.2 or 4 using the tailored parameters $\Delta\phi^* = \Delta\phi_{target}/i$ or $\Delta f^* = \Delta f_{target}/i$ depending on the targeted modulation scheme. The binary values of the ATE sequence $b_{ATE}(kTs)$ correspond directly to the samples $y(kTs)$ taken from the zero-crossed signal $y(t)$ at the chosen sampling rate f_s.

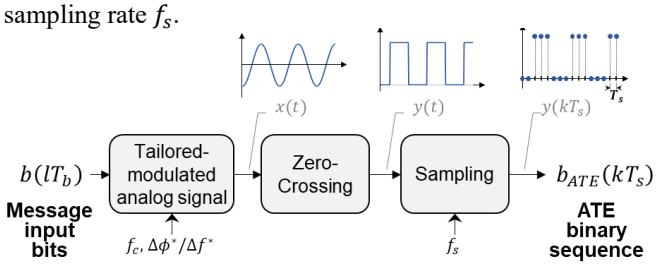

Fig. 6. Determination of the content of the binary sequence that will be stored in the ATE vector memory

B. *Practical application*

To demonstrate the applicability of the proposed solution to various case studies, we have chosen to generate RF test stimuli in the $433MHz$ and $868MHz$ ISM bands, considering both BPSK and MSK modulation formats. The data rate has been arbitrarily fixed to $250kbps$.

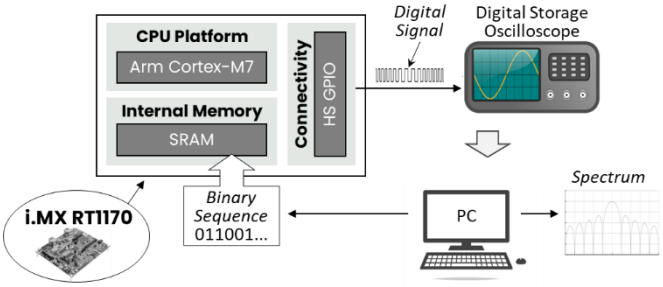

Fig. 7. Experimental setup for the generation of the baseband digital signal

The solution has been implemented on the experimental test bench illustrated in Figure 7, which comprised a microcontroller unit (MCU), a digital-storage oscilloscope (DSO) and a PC. The MCU is a i.MX RT1170 and is used to emulate the operation of a digital tester channel: the Arm-Cortex-M7 core is programmed to read the binary sequence stored in the internal SRAM and output it on a high-speed GPIO (General-Purpose Input/Output) port, where the binary sequence is precomputed on the PC. The signal digital delivered on the GPIO port is sent to the DSO that performs acquisition of the transient waveform; captured data are then transferred to the PC to evaluate spectral content of the generated digital signal (FFT calculation). With this setup, the maximum sampling frequency is $f_{s_{max}} = 498MHz$ and it can be adjusted by step of $\Delta f_s = 3MHz$.

Table I summarizes the computed baseband signal parameters and the selected sampling frequency for the two targeted carrier frequencies and the two modulation formats. For the generation of test stimuli at $433MHz$, the 3rd-order harmonic replica is used. The baseband frequency is therefore set to $f_c = 144.333MHz$, which leads to 70 possible values for f_s comprised between $291MHz$ and $498MHz$. The selected value is $f_s = 483MHz$ with a corruption score of $1.25\ 10^{-4}$ for BPSK, and $f_s = 303MHz$ with a corruption score of $1.21\ 10^{-7}$ for MSK. For the generation of test stimuli at $868MHz$, it is the 5th-order harmonic replica that is used, which gives a baseband frequency $f_c = 173.6MHz$. Among the 51 possible values of f_s between $348MHz$ and $498MHz$, the selected value is $f_s = 420MHz$ with a corruption score of $1.14\ 10^{-4}$ for BPSK, and $f_s = 381MHz$ with a corruption score of $2.06\ 10^{-6}$ for MSK.

TABLE I.
BASEBAND SIGNAL PARAMETERS AND SAMPLING FREQUENCY FOR THE DIFFERENT CASE STUDIES

Parameter	Value			
$f_{c_{target}}$	$433MHz$		$868MHz$	
H_i	H_3		H_5	
f_c	$144.333MHz$		$173.600MHz$	
Mod Type	BPSK	MSK	BPSK	MSK
$\Delta\phi^* / \Delta f^*$	$\pi/3\ rad$	$20.83kHz$	$\pi/5\ rad$	$12.5kHz$
f_s	$483MHz$	$303MHz$	$420MHz$	$381MHz$
$Corr\ Est$ #	$1.25\ 10^{-4}$	$1.21\ 10^{-7}$	$1.14\ 10^{-4}$	$2.09\ 10^{-6}$

Corruption estimator has been computed considering an enlarged bandwidth $EBW = 2 * BW_{99}\%$

V. HARDWARE MEASUREMENT RESULTS

The four case studies were implemented on the experimental test bench. Results for the generation of test stimuli at $433MHz$ are detailed in Figure 8 and 9, which give a global view of the spectrum as well as a close-up view on the baseband spectrum and the selected harmonic replica, for BPSK and MSK respectively. As expected, the global spectrum has a hairy aspect due to the presence of images created by the sampled-time generation process; the shaping by the sin_c function is also visible. Despite the hairy aspect of the global spectrum, the spectral content around the selected harmonic replica exhibits the desired characteristics and is in a good agreement with the theoretical spectrum across all the signal bandwidth, in both cases. This good agreement is obtained thanks to the proper encoding of the digital signal. Indeed, the baseband spectrum presents very different characteristics, as expected from the theoretical analysis of Section II.B (cf. Figure 4).

Results for the generation of test stimuli at $868MHz$ are summarized in Figure 10 and 11, which only show the close-up view around the 5th-order harmonic replica, for BPSK and MSK respectively. Here again in both cases, a good agreement is observed in the signal bandwidth between the experimental spectrum and the expected one. These results confirm the adaptability of the approach that is able not only to cope with different modulation formats, but also to handle different frequency ranges by exploiting different harmonic replicas. In particular, this experiment demonstrates the feasibility of generating a test stimulus at a frequency higher than 3 times the Nyquist rate.

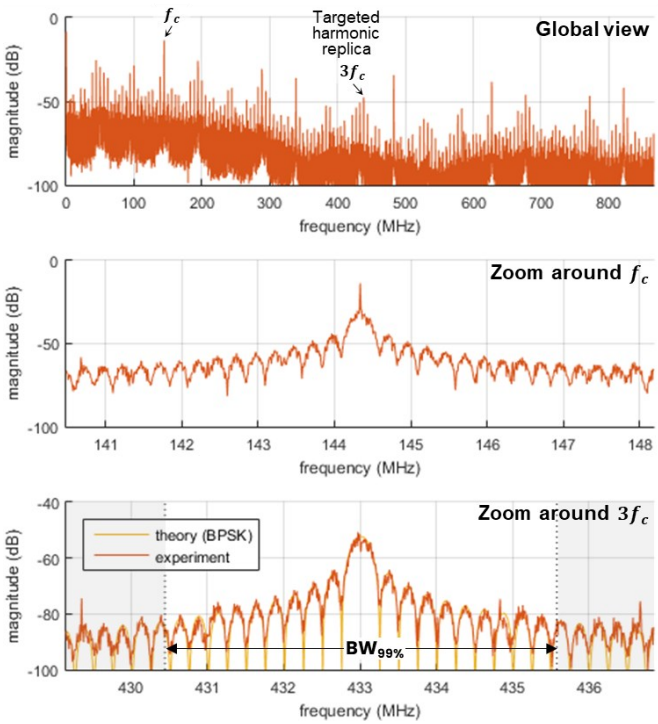

Fig. 8. Experimental spectrum of the digital signal targeting BPSK test stimulus at $433MHz$ using $f_c = 144.333MHz$ and $f_s = 483MHz$

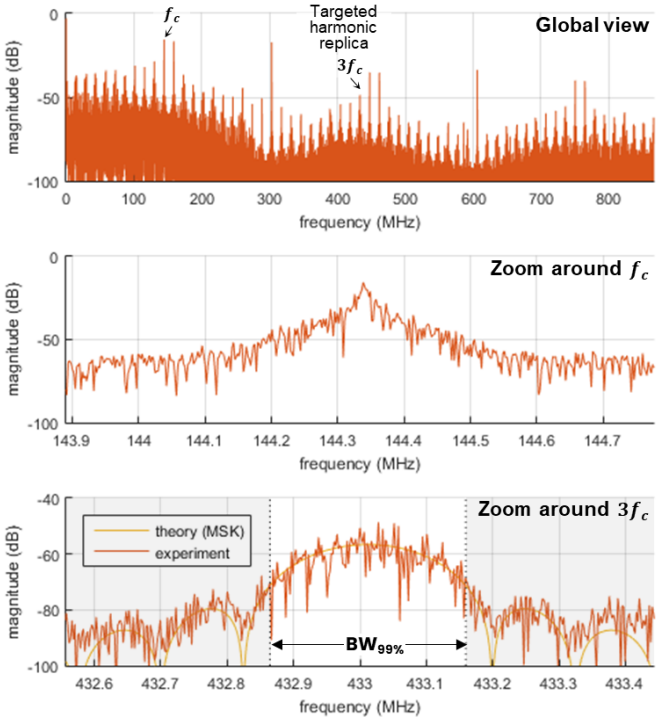

Fig. 9. Experimental spectrum of the digital signal targeting MSK test stimulus at $433MHz$ using $f_c = 144.333MHz$ and $f_s = 303MHz$

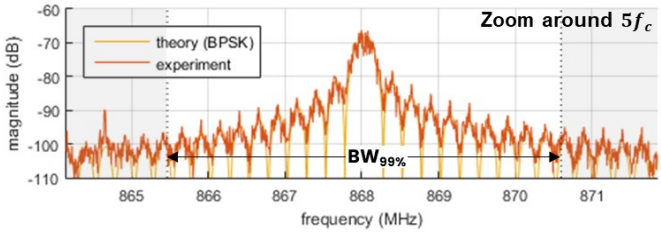

Fig. 10. Experimental spectrum of the digital signal targeting BPSK test stimulus at $868MHz$ using $f_c = 173.6MHz$ and $f_s = 420MHz$

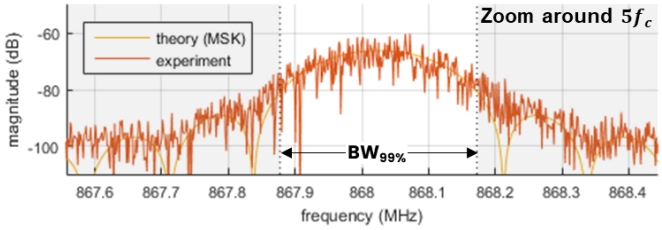

Fig. 11. Experimental spectrum of the digital signal targeting MSK test stimulus at $868MHz$ using $f_c = 173.6MHz$ and $f_s = 381MHz$

VI. Conclusion

In this paper, we have presented a low-cost solution for generating baseband digital signals that encode representative RF signals, as needed to perform sensitivity test of receivers. The approach relies on the exploitation of a harmonic replica of the digital signal in order to reach high frequencies despite the limited sampling capabilities of the test equipment. A generic methodology has been defined which permits to (i) select the order of the harmonic replica depending on the equipment's capabilities (ii) define the proper encoding of the digital signal according to the targeted modulation format and (iii) identify a favorable sampling condition that preserves the spectral quality of the test stimulus in the DUT frequency band. Hardware measurements have demonstrated the validity of the proposed solution and its ability to handle various modulation formats and frequency ranges. Future work will target the practical implementation on an actual ATE, as well as extension to other digital modulation formats.

References

[1] I. Kore et al., "Multi-site test of RF transceivers on low-cost digital ATE,"Proc. IEEE Int'l Test Conference (ITC), pp. 1-10 2011.

[2] C. H. Peng et al., "A novel RF self test for a combo SoC on digital ATE with multi-site applications," Proc. IEEE Int'l Test Conference (ITC), pp. 1-8, 2014.

[3] M. Ishida K. Ichiyama, "An ATE System for Testing RF Digital Communication Devices With QAM Signal Interfaces," IEEE Design & Test, vol. 33, no. 6, pp. 15-22, 2016.

[4] S. David-Grignot et al., "Low-cost phase noise testing of complex RF ICs using standard digital ATE," Proc. IEEE Int'l Test Conference (ITC), pp. 1-9, 2014.

[5] T. Vayssade et al., "EVM measurement of RF ZigBee transceivers using standard digital ATE", Proc. Design, Automation & Test in Europe Conference (DATE), pp. 396-401, 2021.

[6] A. Banerjee et al., "Optimized digital compatible pulse sequences for testing of RF front end modules," Proc. IEEE 16th Int'l Mixed-Signals, Sensors and Systems Test Workshop (IMS3TW), pp. 1-6, 2010.

[7] M. A. Zeidan et al., "Phase-Aware Multitone Digital Signal Based Test for RF Receivers," in IEEE Trans on Circuits and Systems I (TCAS), vol. 59, no. 9, pp. 2097-2110, Sept. 2012.

[8] X. Wang et al., "Low cost high frequency signal synthesis: Application to RF channel interference testing", Proc. IEEE VLSI Test Symp. (VTS), pp. 1-6, 2015.

[9] T. Vayssade et al., "Exploration of a digital-based solution for the generation of 2.4GHz OQPSK test stimuli," Proc. IEEE European Test Symp. (ETS), pp. 1-6, 2021.

[10] K. Tahraoui et al., "Digital generation of single-tone FM/PM test stimuli: a theoretical analysis," Proc. IEEE Latin-American Test Symp. (LATS), pp. 1-6, 2024.

[11] Fuqin Xiong, "Digital Modulation Techniques", Second Edition , Artech, 2006.

[12] F. Amoroso, "The bandwidth of digital data signal," in IEEE Communications Magazine, vol. 18, no. 6, pp. 13-24, Nov. 1980.